Input Voltages and Currents Distortion and Power Factor of Frequency Converters

Oleksandr Zhuk
Dept. of Programmable Electronics, Electrical Engineering and Telecommunications
Admiral Makarov National University of Shipbuilding, NUOS,
Mykolaiv, Ukraine
ak_zhuk@rambler.ru

Dmytro Zhuk
Dept. of Marine Electric Power Systems
Admiral Makarov National University of Shipbuilding, NUOS,
Mykolaiv, Ukraine
vicedirector2012@gmail.com

Oleksii Diakonov
Dept. of Programmable Electronics, Electrical Engineering and Telecommunications
Admiral Makarov National University of Shipbuilding, NUOS,
Mykolaiv, Ukraine
ales.s.dyakonov@gmail.com

***Abstract*— The method of definition input voltages and currents distortion, and also of power factor of frequency converter with DC link and capacitor smoothing filter is developed.**

Keywords— frequency converter, uncontrollable rectifier, voltage source inverter with PWM, total harmonic distortion, power factor.

I. Introduction

Currently modern frequency converters (FC), made according to the scheme "uncontrolled rectifier – pulse-width modulated autonomous voltage inverter" (UR–PWM AVI), are widely used. They provide perfect static and dynamic characteristics of variable frequency drives with a total power of up to several thousand kilowatts, which used, for example, in electric propulsion systems and dynamic positioning of marine vessels and floating structures or in techno-logical installations of offshore drilling platforms [1, 2]. At the same time, the presence of an inverter with DC-link in autonomous and non-autonomous electric power systems (EPS) complicates the nature of electromagnetic processes and the conditions of electromagnetic compatibility (EMC).

The decrease of system power quality in EPS with semiconductor converters is caused by two factors: a phase shift between network voltage and fundamental harmonic of consumed current, and the consumed current higher harmonics presence. The influence of the first factor can be significantly reduced by replacing thyristor-controlled DC drives with AC drives based on FC according to the UR–PWM AVI scheme. However, this aggravates the problems associated with the second factor namely the non-sinusoidality of the FC input current and the corresponding distortions in the supply voltage. These distortions are due to the functioning of two FC circuits with power switches: UR and PWM AVI. PWM AVI generates conductive radio-frequency (RF) electromagnetic interference (EMI) into the supply network because of using PWM at a high carrier frequency of 10-20 kHz. The task of RF EMI reduction for variable frequency drives is the scope of a separate study. The permissible levels of RF EMI are regulated by special international standards (for example, EN 61000-6-1; EN 61000-6-2; EN 55014) and are pro-vided using special lightweight interference filters [3].

In accordance with the state standard GOST 13109-97 adopted in Ukraine, as well as international European standards (EN 50160 and EN 61000-2-2), the satisfactory non-sinusoidality indexes (the coefficients of individual harmonics and THD) of network voltage which is supplied to FC are mainly determined by low-frequency harmonics (up to and including the 40th). Some international standards (EN 61000-3-2 and IEEE 519-1992) also regulate limit levels for such indexes for consumed current [4].

The effect on the network of powerful rectifiers with perfectly smoothed rectified current I_d has been studied quite fully in paper [5].

UR which is a part of an FC with the most common capacitive smoothing filter, mainly operates with a smoothed rectified voltage U_d, as a result the ripple of the rectified current i_d is increased. Due to an increase in the non-sinusoidality of the consumed current, the power factor of FC is decreased and FC EMC performance with respect to the supply network worsens, the study of this mode is of undoubted theoretical and practical interest.

Many manufacturers remove electromagnetic elements such as smoothing chokes and UR input reactors from FC design to reduce its weight, size and cost. In the existing market for electronic components, smoothing chokes and reactors are options and are purchased at an additional cost, which is quite high and makes up 30% of the FC cost [6]. Only after detecting an EMC violation during operation, FCs are additionally equipped with electromagnetic elements which are the part of the UR input and output filters [7, 8].

The voltage and current distortion evaluation of EPS with DC-linked FC is very important for deciding on the use of additional UR input and output filters at the design stage. These questions are actively considered by authors [9, 10, 11]. At the same time, due to the growing power of frequency-controlled electric drives and increasing requirements for their EMC, the advanced methods for calculating the relevant indexes should be further developed and generalized.

A. Research Tasks and Objectives

The purpose of the current work is to obtain generalized analytical expressions and graphical dependencies for determining the non-sinusoidality indexes of input voltages and currents, as well as the power factor of UR with a capacitive smoothing filter. The expressions obtained are necessary for EMC evaluation of FC with a DC link to supply network. Achieving this goal involves solving the following tasks:

1. Development of mathematical model and analysis of electromagnetic processes in UR at various values of the rectified voltage.

2. Harmonic analysis and determination of non-sinusoidality indexes of UR input voltages and currents.

3. Study of the energy characteristics of the DC-linked FC and comparing them for circuits with capacitive and inductive-capacitive smoothing filters.

II. Mathematical model and electromagnetic processes analysis

The generalized circuit of the system "power supply network - frequency converter – asynchronous machine (AM)" and the corresponding equivalent circuit for evaluating the inverter influence on the network are presented in Fig. 1, a, b respectively. In an equivalent circuit, the power supply is represented by a three-phase system of sinusoidal EMFs and short-circuit reactances X_s. The equivalent circuit also includes a matching transformer TR with transformation coefficient $K_T=W_1/W_2$; reactance X_{Fc} is determined from the short circuiting experiment of TR secondary winding. Assume that the UR is made in accordance with a three-phase bridge circuit, and the filter capacitance C_d is large enough so that the rectified voltage U_d contains only a DC component. This assumption allows, in accordance with the compensation theorem, to consider the AVI – AM system as an equivalent EMF $U_{dFc}=U_d\cdot K_T$ referred to the primary transformer winding and placed in the UR load circuit. Instantaneous value of equivalent rectified current is $i_{dFc}=i_d/K_T$.

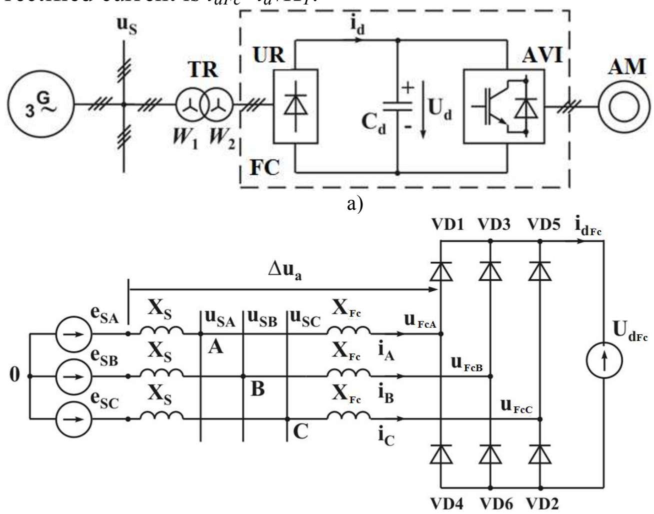

a)

b)

Fig.1.

The analysis is performed for phase A of the system. The instantaneous value of the FC input phase voltage (UR input) u_{Fc} is defined as the difference between the source EMF and the voltage drop Δu_{Fc} across the reactance $X_K=X_s+X_{Fc}$ due to phase current i flow:

$$u_{Fc} = E_m\sin\theta - \Delta u_{Fc}, \qquad (1)$$

where $u_{Fc} = X_K di/d\theta$, $\theta = \omega t$.

Depending on the U_{dFc} value, three UR operation modes are possible, each of which is characterized by a different number of conductive switches on the continuity intervals: mode 2–3, mode 0–2–3 and mode 0–2.

Using the superposition method to analyze the equivalent circuit (Fig. 1, b) at the intervals of UR continuous operation, analytical expressions of u_{Fc} and Δu_{Fc} for each of the operation modes can be obtained. These expressions are presented in Table I.

The waveforms of phase EMF, voltages, and currents at the UR input for the modes mentioned above are presented in Fig. 2, a, b, c respectively. It should be noted that the rectified current i_d in the first mode is continuous, and in the second and third modes is discontinuous.

<u>Mode 2–3.</u> In the expressions for the continuity interval boundaries, the following notations are used: Δ – the shift angle between the natural switching points of the UR switches at idle state and under load, γ – the commutation angle.

The angle Δ can be defined as the difference of the abscissas corresponding to the points of intersection of the phase EMF and voltage [12]:

$$\Delta = \arcsin(U^*_{dFc}/\sqrt{3}) - \pi/6, \qquad (2)$$

Where $U^*_{dFc} = U_{dFc}/\sqrt{3}E_m$ – rectified voltage relative value.

The commutation angle is determined by the equation obtained from the periodicity condition of the rectified current [12]:

$$[1/\sqrt{3}]\cos(\Delta+\gamma/2)\sin(\gamma/2+\pi/3) - U^*_{dFc}[\pi+\gamma]/6 = 0. \quad (3)$$

Based on the analysis of the rectified current waveform, its average value I_{dFc} in fractions of the amplitude of short-circuit current in switching circuit loop is found from the expression

$$\begin{aligned} I^*_{dFc} &= 2I_{dFc}X_K/\left(\sqrt{3}E_m\right) = \\ &= \frac{6}{\pi}\left\{\frac{1}{\sqrt{3}}\left[\frac{2\pi}{3}\sin\left(\frac{\pi}{6}+\Delta+\frac{\gamma}{2}\right)\sin\frac{\gamma}{2}+\right.\right. \\ &+\left[\sqrt{3}\pi/6\right]\cos(\pi/3+\Delta+\gamma)+[\gamma/2]\cos(\Delta+\pi/6)+ \\ &\left.\left.+\sin(\Delta+\gamma/2)\cos(\gamma/2-\pi/6)-\left[U^*_{dFc}/36\right]\left(\pi^2+3\gamma^2+4\pi\gamma\right)\right]\right\} \end{aligned} \qquad (4)$$

The continuous rectified current mode 2–3 corresponds to the condition $U^*_{dFc} < U^*_{dFc\,bgn}$, $U^*_{dFc\,bgn}$ is the value of the rectified voltage (in p.u.) corresponding to the initial discontinuous current that occurs at the boundary of modes 2–3 and 0–2–3, when its minimum value is $i_{d\,\min} = 0$.

Considering that current i_d minima occur at the conduction intervals of two switches and, taking into account, for example, interval 2 (Table I), the condition of the initial discontinuous current can be obtained.

$$i_{d2\min} = i_{2\min} = \frac{1}{X_K}\left(\int_{\frac{\pi}{6}+\Delta}^{\frac{\pi}{6}+\Delta+\gamma}\Delta u_1 d\theta + \int_{\frac{\pi}{6}+\Delta+\gamma}^{\theta_{\min}}\Delta u_2 d\theta\right) = 0, \qquad (5)$$

Where $\theta_{\min}$ – the actual angle which corresponds to the minimum in the considered interval. From the necessary minimum condition $i'_{d2}(0) = 0$ it follows that [12]

$$\theta_{\min} = \arcsin U^*_{dFc} - \pi/6. \qquad (6)$$

Based on (5) and (6) it follows that

$$\begin{aligned} &\left(1/\sqrt{3}\right)\left\{2\sin(\pi/6+\Delta+\gamma/2)\sin\gamma/2+\right. \\ &\left.+\left(\sqrt{3}/2\right)\left[\cos(\pi/3+\Delta+\gamma)-\sqrt{1-U^{*}_{dFc\,bgm}}\right]\right\}+ \\ &+\left[U^*_{dFc}/12\right]\left(\pi+6\Delta+2\gamma-6\theta_{\min}\right)=0 \end{aligned} \qquad (7)$$

TABLE I.

	Interval No	Switch conduct.	θ	u_{FcN}	Δu_{FcN}
Mode 2-3	1	1, 5, 6	$\pi/6+\Delta \le \theta \le \pi/6+\Delta+\gamma$	$U_{dF}/3$	$E_m\sin\theta - U_{dF}/3$
	2	1, 6	$\pi/6+\Delta+\gamma \le \theta \le \pi/2+\Delta$	$[E_m/2]\sin(\theta-\pi/3)+U_{dF}/2$	$[\sqrt{3}/2]\cdot E_m\sin(\theta+\pi/6) - U_{dF}/2$
	3	1, 2, 6	$\pi/2+\Delta \le \theta \le \pi/2+\Delta+\gamma$	$2U_{dF}/3$	$E_m\sin\theta - 2U_{dF}/3$
	4	1, 2	$\pi/2+\Delta+\gamma \le \theta \le 5\pi/6+\Delta$	$[E_m/2]\sin(\theta+\pi/3)+U_{dF}/2$	$[\sqrt{3}/2]\cdot E_m\sin(\theta-\pi/6) - U_{dF}/2$
	5	1, 2, 3	$5\pi/6+\Delta \le \theta \le 5\pi/6+\Delta+\gamma$	$U_{dF}/3$	$E_m\sin\theta - U_{dF}/3$
	6	2, 3	$5\pi/6+\Delta+\gamma \le \theta \le 7\pi/6+\Delta$	$E_m\sin\theta$	0
Mode 0-2-3	1	1, 5, 6	$\pi/6+\Delta \le \theta \le \pi/6+\Delta+\gamma$	$U_{dF}/3$	$E_m\sin\theta - U_{dF}/3$
	2	1, 6	$\pi/6+\Delta+\gamma \le \theta \le \pi/6+\Delta+\gamma+\delta$	$[E_m/2]\sin(\theta+\pi/3)+U_{dF}/2$	$[\sqrt{3}/2]\cdot E_m\sin(\theta+\pi/6) - U_{dF}/2$
	3	–	$\pi/6+\Delta+\gamma+\delta \le \theta \le \theta_1$	$E_m\sin\theta$	0
	4	1, 6	$\theta_1 \le \theta \le \pi/2+\Delta$	$[E_m/2]\sin(\theta-\pi/3)+U_{dF}/2$	$[\sqrt{3}/2]\cdot E_m\sin(\theta+\pi/6) - U_{dF}/2$
	5	1, 2, 6	$\pi/2+\Delta \le \theta \le \pi/2+\Delta+\gamma$	$2U_{dF}/3$	$E_m\sin\theta - 2U_{dF}/3$
	6	1, 2	$\pi/2+\Delta+\gamma \le \theta \le \pi/2+\Delta+\gamma+\delta$	$[E_m/2]\sin(\theta+\pi/3)+U_{dF}/2$	$[\sqrt{3}/2]\cdot E_m\sin(\theta-\pi/6) - U_{dF}/2$
	7	–	$\pi/2+\Delta+\gamma+\delta \le \theta \le \pi/3+\theta_1$	$E_m\sin\theta$	0
	8	1, 2	$\theta_1+\pi/3 \le \theta \le 5\pi/6+\Delta$	$[E_m/2]\sin(\theta+\pi/3)+U_{dF}/2$	$[\sqrt{3}/2]\cdot E_m\sin(\theta-\pi/6) - U_{dF}/2$
Mode 0-2	1	1, 6	$\theta_1 \le \theta \le \theta_2$	$[E_m/2]\sin(\theta-\pi/3)+U_{dF}/2$	$[\sqrt{3}/2]\cdot E_m\sin(\theta+\pi/6) - U_{dF}/2$
	2	–	$\theta_2 \le \theta \le \pi/3+\theta_1$	$E_m\sin\theta$	0
	3	1, 2	$\pi/3+\theta_1 \le \theta \le \pi/3+\theta_2$	$[E_m/2]\sin(\theta+\pi/3)+U_{dF}/2$	$[\sqrt{3}/2]\cdot E_m\sin(\theta-\pi/6) - U_{dF}/2$
	4	–	$\pi/3+\theta_2 \le \theta \le 2\pi/3+\theta_1$	$E_m\sin\theta$	0
	5	2, 3	$2\pi/3+\theta_1 \le \theta \le 2\pi/3+\theta_2$	$E_m\sin\theta$	0
	6	–	$2\pi/3+\theta_2 \le \theta \le \pi+\theta_1$	$E_m\sin\theta$	0

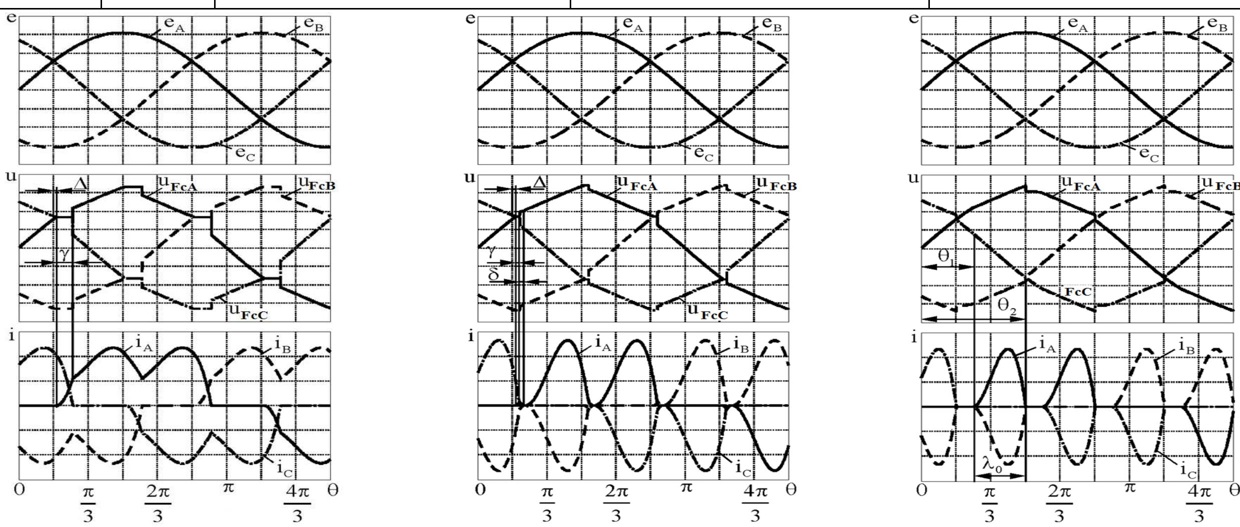

a) b) c)

Fig.2.

Solving (7) it can be obtained that $U^*_{dFc\,bgn} = 0{,}949$.

<u>Mode 0–2–3.</u> The phase current in this mode is continuous in the interval $\theta_1 \le \theta \le \pi/2+\Delta+\gamma$ and is equal to zero at the boundaries of this interval. Therefore

$$i=\frac{1}{X_K}\left(\int_{\theta_1}^{\frac{\pi}{2}+\Delta}\Delta u_4\,d\theta+\int_{\frac{\pi}{2}+\Delta}^{\frac{\pi}{2}+\Delta+\gamma}\Delta u_5\,d\theta\right)=0\,. \qquad (8)$$

The beginning of interval 4 (Table I) is determined from the equation $\theta_1 = \arcsin U^*_{dFc} - \pi/6$.

From (8), we can obtain an equation that implicitly determines the commutation angle γ for the mode 0–2–3, as follows

$$\begin{aligned}&\cos(\theta_1+\pi/6)-\cos(\Delta+2\pi/3)-4/\sqrt{3}\times\\&\times\sin(\Delta+\gamma/2-\pi/6)\sin(\gamma/2)-U^*_{dFc}(\pi/2+\Delta+[2/3]\gamma-\theta_1)=0\end{aligned} \qquad (9)$$

The final value $U^*_{dFc\ end}$ corresponding to the boundary of the modes 0–2–3 and 0–2 is determined from (9) under the condition $\gamma = 0$, i.e.

$$\cos(\theta_1+\pi/6)-\cos(\Delta+2\pi/3)-U^*_{dFc}(\pi/2+\Delta-\theta_1)=0 \quad , (10)$$

where from $U^*_{dFc\ end} = 0{,}958$.

The duration δ of the interval 2 of the conductivity of two switches following the interval 1 of the conductivity of three switches is determined by the expression

$$\begin{aligned} & i(\Delta+\pi/6+\gamma+\delta)= \\ & =\frac{1}{X_K}\left(\int_{\frac{\pi}{6}+\Delta}^{\frac{\pi}{6}+\Delta+\gamma}\Delta u_1 d\theta+\int_{\frac{\pi}{6}+\Delta+\gamma}^{\frac{\pi}{6}+\Delta+\gamma+\delta}\Delta u_2 d\theta\right)=0, \end{aligned} \tag{11}$$

which corresponds to an equation that implicitly determines δ

$$\begin{aligned} & \frac{2}{\sqrt{3}}\sin\left(\Delta+\frac{\pi}{6}+\frac{\gamma}{2}\right)\sin\frac{\gamma}{2}+ \\ & +\sin\left(\Delta+\frac{\pi}{3}+\gamma+\frac{\delta}{2}\right)\sin\frac{\delta}{2}-\frac{U^*_{dFc}}{6}(2\gamma+3\delta)=0. \end{aligned} \tag{12}$$

The average value of the rectified current in the mode 0–2–3 is:

$$\begin{aligned} I^*_{dFc} &= \frac{6X_k}{\pi\sqrt{3}E_m}\int_{\theta_1}^{\frac{\pi}{2}+\Delta+\gamma+\delta} i d\theta = \\ &= [3/\pi]\{(\pi/2-\Delta-\theta_1+\gamma+\delta)\cos(\theta_1+\pi/6)+ \\ & (\gamma+\delta)\sin(\pi/6+\Delta)+[4/\sqrt{3}]\sin(\gamma/2)[\sin(\Delta+\gamma/2)+ \\ & +\delta\cos(\Delta+\gamma/2)]-[\cos(\pi/6+\Delta)-\sin(\pi/6+\theta_1)+ \\ & +[2/\sqrt{3}]\gamma\sin\Delta]-\delta[\cos(\pi/3+\Delta+\gamma+\delta/2)- \\ & -\cos(\pi/3+\Delta+\gamma)]-U^*_{dFc}[0.5(\pi/2+\Delta-\theta_1)^2+ \\ & +(\gamma+\delta)(\pi/2+\Delta-\theta_1)+[2/3]\gamma^2+[4/3]\gamma\delta+0.5\delta^2]\} \end{aligned} \tag{13}$$

Mode 0–2. In this mode, the duration λ_0 of the conduction intervals of the switches two at a time is determined from equation [12]

$$\lambda_0\sin\psi = \cos\psi - \cos(\psi+\lambda_0), \tag{14}$$

where $\psi = \arcsin U^*_{dFc}$.

The beginning and end of interval 1, on which the swithes VD1 and VD6 conduct current (Fig. 2, c), are equal to θ_1 and $\theta_2 = \lambda_0 + \theta_1$ respectively. The average value of the rectified current in mode 0–2 is

$$\begin{aligned} I^*_{dFc} &= \frac{6X_k}{\pi\sqrt{3}E_m}\int_{\theta_1}^{\theta_2} i_1 d\theta = \\ &= \frac{3}{\pi}\left\{(\theta_2-\theta_1)\cos\left(\theta_1+\frac{\pi}{6}\right)-\right. \\ & \left.-2\cos\left(\frac{\theta_2+\theta_1}{2}+\frac{\pi}{6}\right)\sin\left(\frac{\theta_2-\theta_1}{2}\right)-\frac{U^*_{dFc}}{2}(\theta_2-\theta_1)^2\right\} \end{aligned} \tag{15}$$

According to (4), (13) and (15) Fig. 3 shows the universal dependencies for the rectifier: operating characteristic $U^*_{dFc\cdot}=f(I^*_{dFc})$ and load characteristic $U^*_{dFc\cdot}=f(P^*_{dFc})$.

Here $P^*_{dFc\cdot}= P^*_{dFc}/S_{s.c.} = P^*_{dFc}I^*_{dFc\cdot}$ is the relative value of the active load power in fractions of the power of the three-phase short circuit in UR connection terminals: $S_{s.c.} = 3E_m^2/(2X_K)$. The rectifier load is caused by the active power consumed by the AM (the AVI losses are neglected). Therefore, the dependences $U^*_{dFc\cdot}= f(I^*_{dFc})$ and $U^*_{dFc\cdot}= f(P^*_{dFc})$ uniquely determine the mode of UR as a part of FC.

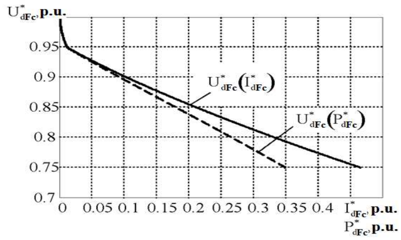

Fig.3.

The values of the rectified current and load power corresponding to $U^*_{dFc\ bgn\cdot}$ And $U^*_{dFc\ end\cdot}$ at the modes boundaries are: $I^*_{dFc\ bgn} = 0{,}011$, $I^*_{dFc\ end} = 0{,}008$, $P^*_{dFc\ bgn\cdot}= 0{,}011$, $P^*_{dFc\ end\cdot}= 0{,}007$.

According to (3) and (9) fig. 4 shows the dependence plot $\gamma = f(U^*_{dFc})$ for modes 2–3 and 0–2–3.

III. FC INPUT VOLTAGES AND CURRENTS NONSINUSOIDALITY INDEXES AND FC ENERGY CHARACTERISTICS MODEL AND ELECTROMAGNETIC PROCESSES ANALYSIS

UR input voltage u_{Fc} non-sinusoidality indexes are determined as a result of a harmonic analysis of the input voltage distortion component Δu_{Fc}.

The relative ν-order (ν = 1, 5, 7, 11, 13…) harmonic complex magnitude as a part of the voltage Δu_{Fc} in fractions of E_m is determined by the expression

$$\Delta\dot{U}^*_{Fc(\nu)} = \frac{2j}{\pi E_m}\int_{\theta_L}^{\theta_L+\pi}\Delta U_{II}(\theta)e^{-j\nu\theta}d\theta, \tag{16}$$

where the integration lower limit is $\theta_L = \pi/6 + \Delta$ for mode 2–3 and 0–2–3; $\theta_L = \theta_1$ for mode 0–2.

Higher-order harmonics (ν = 1, 5, 7, 11, 13…) are identical for u_{Fc} and Δu_{Fc}, therefore

$$\dot{U}^*_{Fc(\nu)} = \Delta\dot{U}_{Fc(\nu)}. \tag{17}$$

For the fundamental harmonic there is a valid expression given below

$$\dot{U}^*_{Fc(1)} = 1-\Delta\dot{U}^*_{Fc(1)}. \tag{18}$$

The relative RMS value of the UR input voltage distortion component is

$$\Delta U^*_{Fc} = \frac{1}{E_m}\left(\frac{1}{\pi}\int_{\theta_L}^{\theta_L+\pi}\Delta U^2_{Fc}(\theta)d\theta\right)^{\frac{1}{2}} \tag{19}$$

The expressions for $\dot{U}^*_{Fc(\nu)}$ (ν = 5, 7, 11, 13 …), and ΔU^*_{Fc} in mode 2–3 and mode 0–2 are presented in Table II. The expressions of mode 2–3 are also valid for the mode 0–2–3 with an error not exceeding 5%, provided that the angle γ is determined in accordance with (9).

Universal dependences of the higher voltage harmonics relative magnitudes $U^*_{dF(\nu)\cdot}= f(P_{dFc})$ (ν = 5, 7, 11, 13 …) and the fundamental harmonic voltage drop $U^*_{dF(1)\cdot}$of at the UR input, obtained on the basis of Table II and expressions (4), (13), (15), are presented in Fig. 5.

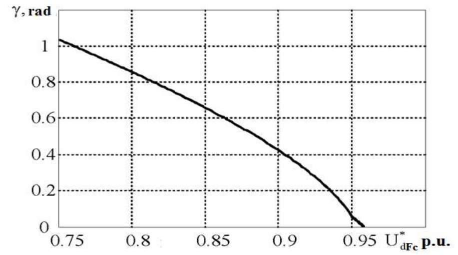

Fig.4.

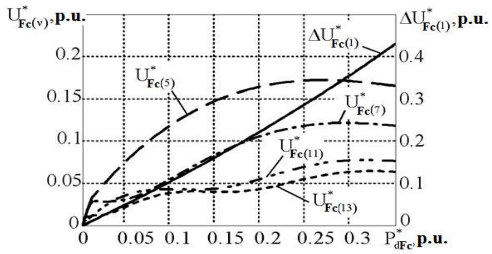

Fig.5.

The higher harmonics relative magnitudes of the current consumed by the FC, and of the voltage on the EPS buses are conveniently found from the expressions given below

$$I^*_{(\nu)} = 2U^*_{Fc(\nu)} \Big/ \left(\sqrt{3}\nu\right); \tag{20}$$

$$U^*_{S(\nu)} = aU^*_{Fc(\nu)}, \tag{21}$$

where $a = X_S/X_K$.

The fundamental harmonic magnitudes of the EPS phase current and voltage are expressed as follows:

$$I^*_{(1)} = 2\Delta U^*_{Fc(1)} \Big/ \sqrt{3}; \tag{22}$$

$$U^*_{S(1)} = \left|1 - \Delta\dot{U}^*_{Fc(1)}\right|. \tag{23}$$

In accordance with domestic and international standards, the voltage non-sinusoidality of the supply network is determined by the coefficients of individual harmonics $K_{US(\nu)}$ and by the THD$_F$ K_{US}, where

$$K_{US(\nu)} = U^*_{S(\nu)} \Big/ U^*_{S(1)} \tag{24}$$

$$K_{US} = \frac{\left(\sum_{\nu=5}^{\infty} U^{*\,2}_{S(\nu)}\right)^{\frac{1}{2}}}{U^*_{S(1)}} = \frac{\left[\left(a\Delta U^*_{Fc}\right)^2 - \left(a\Delta U^*_{Fc(1)}\right)^2 / 2\right]^{\frac{1}{2}}}{U^*_{S(1)}} \tag{25}$$

When $a = 1$ the last expression determines the THD K_{UFs} of the UR input voltage. Fig. 6 shows the graphical dependencies of $K_{UFs} = f(P^*_{dFc})$ and $\Delta U^*_{Fs(1)} = f(P^*_{dFc})$.

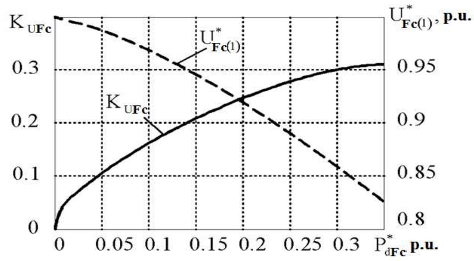

Fig.6.

According to EN 6100-3-2 standart, the coefficients of individual harmonics $K_{I(\nu)}$ and THD K_I are used as indexes of the non-sinusoidality of the FC input phase current; these indexes are determined by the harmonics of the current from expressions similar to (24) and (25).

The main energy characteristic of FC is a power factor χ, which is the ratio of its active power $P^*_{Fc} = P^*_{dFc}$ to apparent power S_{Fc}, determined by the RMS values of the input current i and voltage u_{Fc} of the FC. It is convenient to present the power factor χ as the product of two as follows [5]:

$$\chi = P_{Fc} / S_{Fc} = \lambda \cos\varphi_{(1)}, \tag{26}$$

where

$$\begin{aligned}\varphi_{(1)} &= \angle\left(\dot{U}_{Fc(1)}; \dot{I}_{(1)}\right) = \\ &= Arg\left[1 - \Delta\dot{U}^*_{Fc(1)}\right] - Arg\left[\Delta\dot{U}^*_{Fc(1)} / j\right]\end{aligned} \tag{27}$$

$$\lambda = \left[\left(1 + K^2_{UFc}\right)\left(1 + K^2_I\right)\right]^{-\frac{1}{2}} \tag{28}$$

In accordance with expressions (20) - (28) and Table II the dependencies $\chi = f(P^*_{dFc})$, $\lambda = f(P^*_{dFc})$, $\cos\varphi_{(1)} = f(P^*_{dFc})$, and $K_I = f(P^*_{dFc})$ for a converter with a capacitive smoothing filter are shown in fig. 7.

TABLE II.

Mode 2-3	$\dot{U}^*_{Fc(\nu)} = \frac{1}{\pi} e^{-j\nu\left(\Delta + \frac{\pi}{6}\right)} \left(1 - 2e^{-j\nu\frac{2\pi}{3}} - e^{-j\nu\frac{\pi}{3}}\right) \left\{ \frac{U^*_{dFc}}{\sqrt{3}\nu} \left(e^{-j\nu\left(\gamma + \frac{2\pi}{3}\right)} - 1\right) e^{j\nu\frac{2\pi}{3}} + \frac{j}{2} \left[\frac{e^{-j(\nu-1)\frac{\pi}{3}} - e^{-j(\nu-1)\gamma}}{\nu - 1} e^{-j\left(\frac{\pi}{6} - \Delta\right)} - \frac{e^{-j(\nu+1)\frac{\pi}{3}} - e^{-j(\nu+1)\gamma}}{\nu + 1} e^{j\left(\frac{\pi}{6} - \Delta\right)} \right] \right\}$
	$\Delta\dot{U}^*_{Fc(1)} = \frac{1}{2\pi} \left[\pi + 3\gamma + 3\sin\left(\frac{\pi}{3} - \gamma\right) e^{-j(2\Delta + \gamma)} \right] - \frac{2\sqrt{3}}{\pi} U^*_{dFc} e^{-j\left(\Delta + \frac{\gamma}{2}\right)} \sin\left(\frac{\pi}{3} + \frac{\gamma}{2}\right)$
	$\Delta U^*_{Fc} = \frac{1}{\sqrt{\pi}} \left\{ \frac{3}{4} \left[\gamma + \frac{\pi}{3} + \cos(2\Delta + \gamma) \sin\left(\frac{\pi}{3} - \gamma\right) \right] - 2\sqrt{3} U^*_{dFc} \cos\left(\Delta + \frac{\gamma}{2}\right) \sin\left(\frac{\gamma}{2} + \frac{\pi}{3}\right) + \frac{1}{2} U^{*\,2}_{dFc} (\gamma + \pi) \right\}^{\frac{1}{2}}$
Mode 0-2	$\dot{U}^*_{Fc(\nu)} = \frac{\sqrt{3}}{2\pi} \left(e^{j\nu\frac{3\pi}{3}} - 1\right) \cdot \left\{ j \left[\frac{e^{-j(\nu-1)\theta_2} - e^{-j(\nu-1)\theta_1}}{\nu - 1} e^{j\frac{\pi}{6}} - \frac{e^{-j(\nu+1)\theta_2} - e^{-j(\nu+1)\theta_1}}{\nu + 1} e^{-j\frac{\pi}{6}} \right] + \frac{2U^*_{dFc}}{\nu} \left(e^{-j\nu\theta_2} - e^{-j\nu\theta_1}\right) \right\}.$
	$\Delta\dot{U}^*_{Fc(1)} = \frac{3}{4\pi} \left\{ \left[2(\theta_2 - \theta_1) - je^{-j\frac{\pi}{3}} \left(e^{-j2\theta_2} - e^{-j2\theta_1}\right) \right] + 4U^*_{dFc} e^{-j\frac{\pi}{6}} \left(e^{-j\theta_2} - e^{-j\theta_1}\right) \right\}$
	$\Delta U^*_{Fc} = \left\{ \frac{1}{\pi} \left[\frac{3}{4} \left[(\theta_2 - \theta_1) - \cos\left(\theta_2 + \theta_1 + \frac{\pi}{3}\right) \sin(\theta_2 - \theta_1) \right] - 6U^*_{dFc} \sin\left(\frac{\theta_2 + \theta_1}{2} + \frac{\pi}{6}\right) \sin\frac{\theta_2 - \theta_1}{2} + \frac{3}{2} U^{*\,2}_{dFc} (\theta_2 - \theta_1) \right] \right\}^{\frac{1}{2}}$

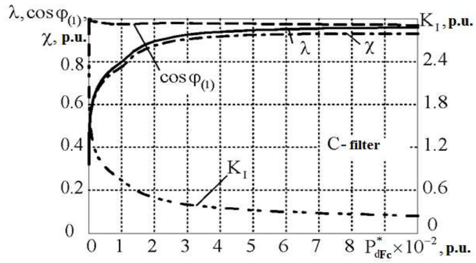

Fig.7.

For comparison, Fig. 8 shows similar dependencies for inductive-capacitive filter. These dependencies are calculated by the method [5] for a perfectly smoothed rectified current.

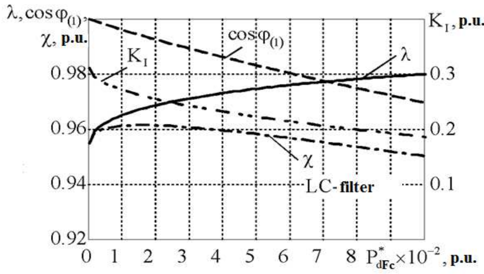

Fig.8.

When assessing the impact on the power supply network, the relative values of the FC active load power P^{*}_{dFc} are conveniently expressed using practical quantities characterizing the circuit and its elements:

$$P^{*}_{dFc} = \frac{3E_m^2}{2X_K} = b\overline{X}_S + \overline{u}_{s.c.}, \quad (29)$$

Where $b = S_{Fc}/S_S$ – the ratio of the installed powers of the FC and the supply network (generator); $\overline{X}_S$ and $\overline{u}_{s.c.}$ – the value of the short circuit reactance of the network and the short circuit voltage of the converter in p.u. respectively.

If a synchronous generator is used as the primary source of electrical energy, then $\overline{X}_S = 0{,}1 \div 0{,}15$ p.u.; with matching transformer $\overline{u}_{s.c.} = 0{,}03 \div 0{,}05$.

Thus, when, for example, the FC power is less than 10% of the source power, i.e. $b = S_{Fc}/S_S \le 0{,}1$ and the rectifier is connected directly to the buses of the EPS ($\overline{u}_{s.c.} = 0$), then $P^{*}_{dFc} \le 0{,}01$..

In this case, when a capacitive smoothing filter is used, the UR operates in discontinuous current i_d mode and the energy characteristics of the FC rapidly deteriorate.

According to fig. 7, the value of the power factor χ can decrease to 0.5 due to an increase in the current consumption THD K_I, while the current reaches 1.5 p.u. (150%).

The analysis of dependencies presented in Fig. 8 shows that in similar modes when using an inductive-capacitive smoothing filter, the value of the FC power factor remains high enough ($\chi \ge 0{,}95$) with a relatively small distortion of the input current waveform ($K_I \le 0{,}3$).

From fig. 7 it follows that an increase in the power factor ($\chi \ge 0{,}9$) with a simultaneous decrease in the distortion of the consumed current ($K_I \le 0{,}35$) is possible for the FC circuit with a capacitive filter, if FC operation mode is ensured at $P^{*}_{dFc} \ge 0{,}03$. From (29) it follows that for this purpose, the FC must be connected to the network through a transformer or line reactors when

$$\overline{u}_{s.c.} \ge 0{,}03 - b\overline{X}_S. \quad (30)$$

IV. CONCLUTIONS

A method for the analysis of electromagnetic processes is proposed, and the characteristic modes of the input uncontrolled rectifier of the frequency converter with a capacitive smoothing filter are investigated.

Generalized analytical expressions and graphical dependencies are obtained for determining the non-sinusoidality indexes of input voltages, currents and power factor of a DC-linked frequency converter.

The calculated coefficients for the practical improvement of the electromagnetic compatibility of the frequency converter with the network are determined.

REFERENCES

[1] D.Kumar, F.Zare, “Comprehensive Review of Maritime Microgrids: System Architectures, Energy Efficiency, Power Quality and Regulations.” IEEE Access, vol. 7,no. 99, pp. 1–11, 2019.

[2] Siemens AG. “The Guide of Marine Frequency Converters. Marine Equipment”. Available online: https://www.siemens.com.tr/i/Assets/Endustri/motorvesurucuteknolojileri/marine/MarineFrequency-Converters.pdf (accessed on 28 April 2016).

[3] Cesar Bocchiola, “Design of the Inverter output filter for Motor Drives with IRAMS Power Modules”, Application Note AN-1095, International rectifier.

[4] A. Zharkin, V. Novskiy, S. Palachov, "Regulation of the electric energy quality. Analysis of Ukrainian and European legislative acts and regulatory technical documents". Institute of Electrodynamics of the National Academy of Sciences of Ukraine in Kyiv, 167 p., 2010. ISBN 978-966-02-5742-9.

[5] Glitternik S.R. “Electromagnetic processes and modes of powerful static converters”, Leningrad: Science, 1968, 308 p.

[6] K. Armstrong, "EMC design of high-frequency power “switchers” and “choppers” - The EMC benefits of LF mains isolating transformers, plus noisesuppression for “floating” power networks and “floating” electronics". The EMC Journal, Issue 104, pp. 30-42, Jan. 2013.

[7] Volkov I.V., Akinin K.P., Isakov G.V. “Comparative analysis of filtering methods for currents consumed by rectifier plants”, Technical electrodynamics. No. 4, p. 21–26, 1999.

[8] F. Leferin, “Preventing on-board power supply problems.” Available online: https://www.nedap-uv.com/uploads/News%20and%20Events/Preventing%20power%20supply%20problems%20onboard%20ships%20long%20version%20%20180423.pdf (accessed on 19 Jan 2020).

[9] Kharitonov S.A. “Analysis of electromagnetic processes in the “magnetoelectric generator - controlled rectifier” generation system”, Proceedings "Energy Saving, Electrical Equipment, Automation of River Ships and Industrial Enterprises." Novosibirsk: NSAWT, p. 96–113, 1997.

[10] Firago BI, Medvedev KM, Pawlaczyk L. Research of input currents of the “Frequency converter asynchronous motor” system in the regime of discontinuous currents and supply voltage asymmetry, Technical electrodynamics.Thematic issue of the problem of modern electrical engineering, 2006. – Part.1– p.29 –35.

[11] M. Artemenko, V. Mykhalskyi, S. Polishchuk,"Definition of apparent power of three-phase power supply system as a theoretical basis for development of energy-efficient shunt active filters", in Technical Electrodynamic, Issue 2, pp. 25-34, 2017.

[12] O Zhuk, “Influence on the supply network of frequency converters with a DC link”, Technical electrodynamics. Thematic issue of power electronics and energy efficiency, 2006. – Part.5 – p. 42 – 46.